RSC Advances

ROYAL SOCIETY OF CHEMISTRY

www.rsc.org/advances

Cite this: DOI: 10.1039/c0xx00000x

www.rsc.org/xxxxxx

PAPER

Electron induced ionization of C_3 to C_6 ethanoates

Jaspreet Kaur, Rahla Naghma and Bobby Antony*

Received (in XXX, XXX) Xth XXXXXXXXX 20XX, Accepted Xth XXXXXXXXX 20XX
DOI: 10.1039/b000000x

The present article reports calculation of electron impact total ionisation cross sections for C_3 to C_6 ethanoates for the energy range from ionisation threshold of the target to 5000 eV. The spherical complex optical potential and complex scattering potential ionisation contribution methods are employed to calculate the cross sections. The results presented here show consistent variation with previous measurements and theoretical values, wherever available. The dependence of isomeric effect on the ionisation cross section is also studied. Plot for the peak of ionisation cross section against the square root of the ratio of polarisability to ionisation potential and with the number of carbon atoms in each target, exhibits strong correlations. Polarisabilities of C_5 and C_6 ethanoates have been estimated from the correlation plot.

I. Introduction

Electron impact ionisation cross-sections for molecules are required in various arenas of applied science and technology viz., modelling of electrical discharges, semiconductor processing, gas lasers, fluorescent lighting, the upper atmosphere, the aurora, and the interstellar medium [1]. However, there are multitudes of molecules for which electron impact ionisation cross sections are still scarce and restricted over a limited energy range. In the present work, the electron impact total ionisation cross section for the ethanoate molecules namely methyl ethanoate (CH_3COOCH_3), ethyl ethanoate ($CH_3COOC_2H_5$), propyl ethanoate (n-$CH_3COOC_3H_7$), iso-propyl ethanoate (iso-$CH_3COOC_3H_7$), butyl ethanoate (n-$CH_3COOC_4H_9$), iso-butyl ethanoate (iso-$CH_3COOC_4H_9$), secondary butyl ethanoate (sec-$CH_3COOC_4H_9$) and tertiary butyl ethanoate (tert-$CH_3COOC_4H_9$) are reported. The presence of methyl ethanoate in the interstellar medium (ISM) has been recently reported by Tercero *et al* [2] using the IRAM 30-m radio telescope employed to explore the Orion constellation. Methyl ethanoate are assumed to be formed in the star forming regions by the reaction between CH_3O and CH_3CO radicals, according to the gas grain warm-up chemical model postulated by Garrod, Weaver and Herbst [3]. Moreover, methyl ethanoate is considered to be the most widely reported and detected non cyclic isomer of $C_3H_6O_2$. Such compounds are also proposed to be found within the ice layers on ISM dust grains [3]. The formation mechanism of methyl ethanoate is expected to be similar to that of methyl methanoate, acetic acid and methanol [4]. The presence of methyl ethanoates in the ISM enhances the possibility of finding higher members of the ethanoate family in such environments. Therefore, the modelling of such environments requires ionisation cross sections as preliminary requisite. Despite this, there is paucity of electron collision data on most of the ethanoate molecules. In 1966, the group of Harrison [5] reported the total ionisation cross section for methyl and ethyl ethanoate at 75 eV for the first time. About four decades later, Hudson *et al* [6] measured the absolute electron impact ionisation cross sections of C_2 to C_6 methanoates and C_3 to C_7 ethanoates from 15 to 285 eV. Along with their measurements, they also reported the calculated maximum total ionisation cross section using Binary Encounter Bethe (BEB) method of Kim and Rudd [7-8]. Later, a revised BEB data over the entire energy range was reported by Bull *et al* [10]. Other than the above dataset, no previous measurement or calculation were found in the literature to the best of our knowledge. The present results are also compared with the unpublished results obtained using Deutsch-Märk (DM) formalism [9]. The dearth of electron impact cross section data for these molecules has motivated us to perform the present calculations.

The molecular structures of the targets studied here are presented in Fig. 1. The energy regime of the present calculation is from ionisation threshold of the target to 5 keV. Previous results for these targets have been reported up to 300 eV only. Therefore, electron impact total ionisation cross section for these molecules over such a wide energy range (11-5000 eV) is presented for the first time. The spherical complex optical potential (SCOP) method [11-17] and group additivity rule (GAR) [11] is employed to calculate the total inelastic cross sections for the ethanoates. A semi-empirical approach called complex scattering potential-ionisation contribution (CSP-ic) method [11-17] is used to deduce the total ionisation cross section of the molecule. A detailed discussion on SCOP, GAR and CSP-ic methods are presented in the next section and references therein. The present results are compared with the measurements of Hudson *et al* [6] and the theoretical data using BEB [7-8] and DM [9] formalisms. A reasonable agreement is observed between the present results and the previous available values for all the targets studied in this work. The isomeric effect on electron impact cross section for propyl and butyl ethanoates are also investigated in this article. In addition to the ionisation cross sections, the polarisability volumes for C_5 and C_6 ethanoates are also estimated using the correlation plot between the maximum ionisation cross section and the square root of the ratio of polarisability to ionisation potential for a number of molecules.

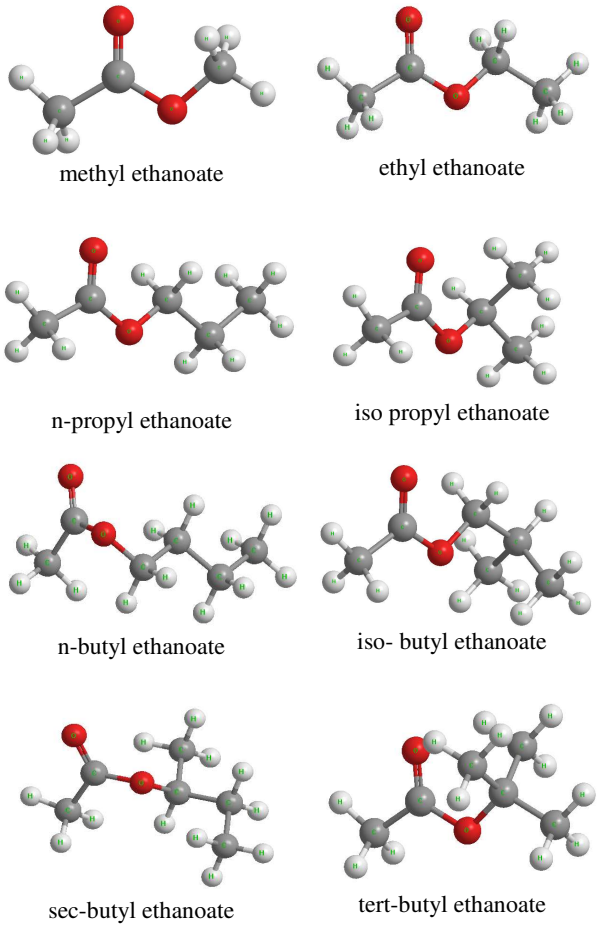

Fig. 1: Structure of targets studied.

II. Theoretical Methodology

This section elucidates the computational procedure adopted to calculate the total ionisation cross sections for the ethanoate molecules by electron scattering. Since the targets studied here are quite large and complex as illustrated in Fig.1, the group additivity rule (GAR) [11] is implemented to evaluate the total inelastic cross section. In GAR [11], different scattering centres are considered in a single molecule, which are assumed to scatter the incoming electron independently. Thus for each scattering centre, independent inelastic contributions are calculated separately using the single centre SCOP formalism [11-17]. Then the total inelastic cross section for the molecule is obtained by adding the contribution from each centres. The total ionisation cross section is then evaluated from the total inelastic cross section by the semi-empirical CSP-ic method [11-17].

Distinct scattering centres of a molecule are chosen depending upon the geometry of the molecule. For all the targets studied in this work, hydrogen atoms attached to a carbon atom always formed one group, while the COO functional group acts as another independent scatterer. Sum of the inelastic cross section of each scattering centres of a given molecule gives the molecular total inelastic cross section (Q_{inel}). For example, in case of CH_3COOCH_3, three scattering centres were assumed: two for each -CH_3 group and one for the COO functional group. Thus, the total inelastic cross section for the molecule, $Q_{inel}(CH_3COOCH_3) = Q_{inel}(CH_3\text{-}) + Q_{inel}(COO) + Q_{inel}(\text{-}CH_3)$.

The interaction dynamics between the incoming electron and each scattering centre is represented by a complex optical potential. This complex potential has the form,

$$V_{opt}(r,E_i) = V_R(r) + iV_I(r,E_i) \quad (1)$$

where the first term takes into account the real static, exchange and polarization potentials and second imaginary term constitutes the absorption effects during the scattering event. These potentials are functions of incident electron energy (E_i) and radial distance between the incident electron and the scattering centre(s). The complex potential given in equation (1) is designed as a function of target parameters and target charge density. The ionisation potentials used in the present work are listed in Table 1. The bond lengths of C-H and C=O of methyl ethanoate are taken from CCCBDB [20]. The correct representation of target charge density is an important prerequisite to obtain accurate potential terms. In the present work we have employed parametrized Hartree-Fock wave function given by Cox and Bonham [21] to compute the target charge density and static potential for each group in a molecule. The parameter free Hara's 'free electron gas exchange model' [22] and correlation-polarization potential given by Zhang *et al* [23] are employed for the exchange potential and polarization potential respectively. The imaginary part of equation (1), called the absorption potential, accounts for the total loss of flux into the inelastic channels like electronic excitation and ionisation. The well-known quasi-free model potential given by Staszewska *et al* [24] is applied for the imaginary part. This absorption potential does not include the vibrational and rotational excitation terms. This is justified since these potentials are important only at very low incident energies and do not significantly contribute to the total cross section in the energy range of present interest.

Table 1 Target properties.

Target	IP (eV)
methyl ethanoate (CH_3COOCH_3)	10.25
ethyl ethanoate ($CH_3COOC_2H_5$)	10.01
n-propyl ethanoate ($CH_3COOC_3H_7$)	10.04
iso-propyl ethanoate (iso-$CH_3COOC_3H_7$)	9.99
n-butyl ethanoate ($CH_3COOC_4H_9$)	10.01
sec-butyl ethanoate (sec-$CH_3COOC_4H_9$)	9.91
iso-butyl ethanoate (iso-$CH_3COOC_4H_9$)	9.90
tert-butyl ethanoate (tert-$CH_3COOC_4H_9$)	9.95

The complex optical potential given in eqn (1) is then incorporated in the Schrödinger equation to find its solution by partial wave analysis. The solution of the radial part of Schrödinger equation for each scattering centre is obtained in terms of complex phase shifts. These phase shifts contain the signature of the scattering event, which are unique to a particular interaction. Thus, various cross sections can be evaluated employing these phase shifts through standard equations [12]. The total inelastic cross section (Q_{inel}) for a molecule is obtained

as the sum of the Q_{inelSC} for the constituent centres.

$$Q_{inel}(E_i) = \sum Q_{inelSC}(E_i) \quad (2)$$

The next task is to deduce total ionisation cross section (Q_{ion}) from Q_{inel}. For this purpose the semi empirical CSP-ic method [11-17] is employed. Since the Q_{inel} do not contain rotational or vibrational excitations, it can be divided into discrete and continuum contributions as,

$$Q_{inel}(E_i) = Q_{exc}(E_i) + Q_{ion}(E_i) \quad (3)$$

The quantities Q_{ion} and total electronic excitation cross section (Q_{exc}) can be measured independently in an experiment and thus the present results can be verified. Also, Q_{ion} has much relevance than Q_{inel} to applied sciences. Even though Q_{inel} and Q_{exc} values are obtained in our calculation, we have reported only Q_{ion} in the present article. To derive Q_{ion} from Q_{inel}, we define an energy dependent ratio of cross sections,

$$R(E_i) = \frac{Q_{ion}(E_i)}{Q_{inel}(E_i)} \quad (4)$$

such that, $0 < R < 1$. The functional form of R is [11-14],

$$R(E_i) = 1 - f(U) = 1 - C_1\left(\frac{C_2}{U + a} + \frac{\ln(U)}{U}\right) \quad (5)$$

Here, U is a dimensionless variable defined through, $U=E_i / I$, where I is the ionisation potential of the target molecule. As the incident energy increases above ionisation threshold of the target, the ratio R increases rapidly and finally approaches unity at very high energies (>500 eV). This is due to the fact that the excitation falls off quickly due to its low threshold and ionisation contribution increases steadily since infinite number of channels are open as energy increases above I. The second term of equation (5) within bracket corresponds to the fall in excitation due to the dipole transitions, which varies as $ln\ (U)/U$ at high energies. The first term in bracket gives better energy dependence at low and intermediate energies ensuring a balanced description of R at all the energies. Equation (5) involves three unknown parameters C_1, C_2 and a, which are dimensionless and depend on target properties and the boundary conditions implied. The boundary conditions defining this ratio are given by,

$$R(E_i) = \begin{cases} 0, & for \quad E_i \le I \\ \cong 1, & for \quad E_i >> E_p \\ R_p, & at \quad E_i = E_p \end{cases} \quad (6)$$

where R_p stands for the value of ratio at which Q_{inel} reaches its peak and E_p is the corresponding incident electron energy. The first and second conditions are trivial. Below the ionisation threshold of the target, the molecule will not get ionised and hence the ratio will be zero. At very high energies the ratio approaches unity as the excitation dies off quickly and hence most of the inelastic part will be of ionisation only. However, the second condition is empirical and was established after studying many literatures and investigating various well known targets. The ionisation cross section curve commences at the ionization threshold of the target. Thereafter, it rises to achieve a maximum value referred to as maximum ionisation cross section and falls beyond the peak with increasing energy. This is the general trend of the ionisation cross section curve. Turner *et al* [25] and Karwasz *et al* [26] observed that the ratio of Q_{ion} to Q_{inel} (R_p) at the peak (equation 6) lies in between 70 to 80%. This is an empirical condition based on several experimental and theoretical studies done on various stable targets like Ne, Ar, O_2, CH_4, etc. [27, 28,29]. The higher limit of 80% is observed for only those atoms with higher ionisation potential (>15 eV) like inert gases. The ionisation potential of all the ethanoates studied here is around 10 eV and hence it is justified in using the lower limit of 70%. This value of R_p may introduce an uncertainty of about 10% from its mean value. However, using a constant value makes our methodology consistent and reproducible. The parameters C_1, C_2 and a calculated using these boundary conditions are tabulated in Table 2. The methodology adopted here is not rigorous, but is capable of producing a good estimate of Q_{ion} within a reasonable uncertainty as required by the atomic and molecular physics community.

Table 2: Parameters used in equation (5) to evaluate R (E_i)

Target	a	C_1	C_2
methyl ethanoate	10.253	-1.321	-8.521
ethyl ethanoate	10.413	-1.324	-8.619
n-propyl ethanoate	10.476	-1.326	-8.656
iso-propyl ethanoate	10.427	-1.325	-8.627
n-butyl ethanoate	10.476	-1.326	-8.656
sec-butyl ethanoate	10.455	-1.325	-8.644
iso-butyl ethanoate	10.455	-1.325	-8.644
tert-butyl ethanoate	10.483	-1.326	-8.661

III. Results and Discussions

The comparison of the present electron impact total ionisation cross sections for the ethanoates are presented in Figs 2-5 with the only available measurements of Hudson *et al* [6] and theoretical data computed by the same group using BEB method [10]. The unpublished data using DM formalism [18] are also plotted. The numerical values obtained are tabulated in Table 3 and Table 4 for ready reference. A comparative study of Q_{ion} for all the ethanoates of the present study is performed in Fig 6. Figure 7 depicts the correlation between the maximum of ionisation cross section versus square root of the ratio of polarisability to ionisation potential of methyl and ethyl ethanoates along with aldehyde, ketone and cycloalkane from previously reported work [12]. We have used the same correlation plot to compute the polarisabilities of C_5 and C_6 ethanoates, since polarisability volumes were not available for these molecules in the literature. The polarisability volumes of higher ethanoates estimated in the present work are tabulated in Table 5. In Table 6, we have compared the peak of present ionisation cross section with the measurements of Hudson *et al* [6], Harrison *et al* [5] and theoretical BEB values by Bull *et al* [10]. A plot of the maximum total ionisation cross section for the ethanoates with the number of carbon atoms contained in the molecule is presented in Fig 8.

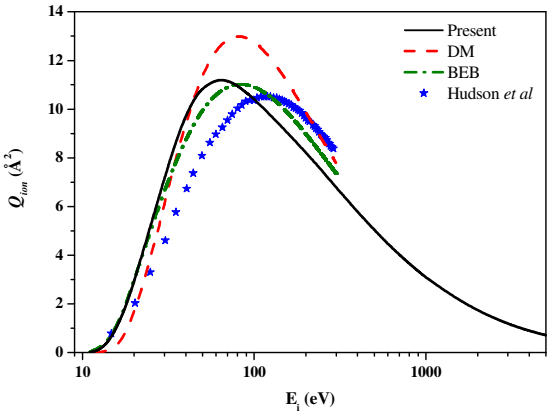

Fig 2. Q_{ion} for CH_3COOCH_3 in Å^2

Figure 2 shows the electron impact total ionisation cross sections for CH_3COOCH_3 molecule along with the experimental values of Hudson et al. [6] and theoretical data due to BEB [10] and DM [18] calculations. The present Q_{ion} retraces the experimental data points at incident electron energies near the threshold, thereafter it is found to slightly overestimate the experimental curve. Beyond the peak position the present results cross over and fall below the measured values. Although the shape and magnitude of the present and experimental ionisation curves are quite similar, the peak position of the present Q_{ion} is shifted towards the lower energy side. The DM results [18] show good agreement with the present Q_{ion} at low electron impact energies up to 50 eV and beyond that the DM [18] values significantly overestimate the present data, experimental values of Hudson *et al* [6] and BEB data given by Bull *et al* [10]. Also, the peak position of the present curve falls before the DM [18] curve. However, the comparison of the present results with BEB data [10] is quite satisfactory over the considered energy range.

In Fig 3, the present total ionisation cross sections for $CH_3COOCH_2CH_3$ are compared with the available measurement and theoretical data. The comparison for ethyl ethanoate shows similar trend as observed in the case of methyl ethanoate. Present Q_{ion} show good accord with the measurements of Hudson *et al* [6] in term of shape of the ionisation curve, with peak position consistently lying at lower energy than the experimental maximum. The agreement between the present Q_{ion} and the DM [18] data is quite good up to 50 eV and beyond that energy DM data rises sharply overestimating all the other data to give a maximum of 16.56 Å^2 at 80 eV. The comparison between the present and BEB data [10] is very good at energies near the threshold and beyond the peak. However, around the peak position BEB values [10] are quite lower than the present Q_{ion}. Ethyl ethanoate has an additional CH_2 group than methyl ethanoate and hence the higher magnitude of cross section in the latter case. However, the peak position remains nearly the same as they have close ionisation thresholds.

Table 3: Total ionisation cross sections for C_3 to C_5 ethanoate molecules in Å^2.

E_i (eV)	methyl ethanoate	ethyl ethanoate	propyl ethanoate	iso-propyl ethanoate
11	0	0.02	0.02	0.02
12	0.05	0.13	0.15	0.12
13	0.18	0.37	0.42	0.34
14	0.38	0.73	0.82	0.68
15	0.65	1.21	1.33	1.12
20	2.64	4.37	4.72	4.16
25	4.81	7.58	8.1	7.36
30	6.7	10.21	10.86	10.1
35	8.25	12.2	12.94	12.29
40	9.4	13.54	14.38	13.91
50	10.7	14.8	15.91	15.73
60	11.22	15.11	16.36	16.43
80	11.19	14.62	15.98	16.38
100	10.78	13.83	15.24	15.79
200	8.6	10.72	12.03	12.57
300	7.03	8.75	9.93	10.3
400	5.96	7.42	8.48	8.74
500	5.18	6.45	7.41	7.6
600	4.58	5.72	6.58	6.73
700	4.11	5.13	5.93	6.04
800	3.72	4.66	5.39	5.47
900	3.4	4.27	4.94	5.01
1000	3.13	3.93	4.56	4.61
2000	1.75	2.2	2.58	2.59
3000	1.2	1.51	1.78	1.78
4000	0.9	1.14	1.34	1.33
5000	0.71	0.9	1.06	1.06

Table 4: Total ionisation cross sections for butyl ethanoate molecules and its isomers in Å^2.

E_i (eV)	butyl ethanoate	sec-butyl ethanoate	iso-butyl ethanoate	tert-butyl ethanoate
11	0.03	0.03	0.03	0.03
12	0.19	0.17	0.18	0.2
13	0.53	0.46	0.51	0.54
14	1.03	0.9	1.01	1.05
15	1.67	1.48	1.64	1.7
20	5.88	5.33	5.86	5.95
25	10.07	9.34	10.09	10.18
30	13.48	12.74	13.53	13.62

35	16.02	15.42	16.14	16.23
40	17.74	17.34	17.91	18
50	19.5	19.44	19.68	19.68
60	19.98	20.2	20.13	20.1
80	19.42	20.01	19.55	19.54
100	18.43	19.25	18.6	18.47
200	14.37	15.11	14.45	14.32
300	11.78	12.32	11.84	11.72
400	10.02	10.41	10.06	9.96
500	8.74	9.03	8.76	8.68
600	7.75	7.98	7.77	7.7
700	6.97	7.15	6.98	6.92
800	6.33	6.48	6.34	6.29
900	5.8	5.93	5.81	5.77
1000	5.35	5.45	5.35	5.32
2000	3.02	3.05	3.02	3.01
3000	2.08	2.09	2.08	2.08
4000	1.56	1.57	1.56	1.56
5000	1.24	1.25	1.24	1.24

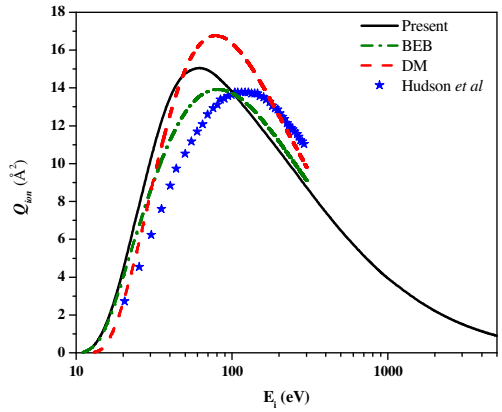

Fig 3. $\boldsymbol{Q_{ion}}$ for $CH_3COOCH_2CH_3$ in Å^2

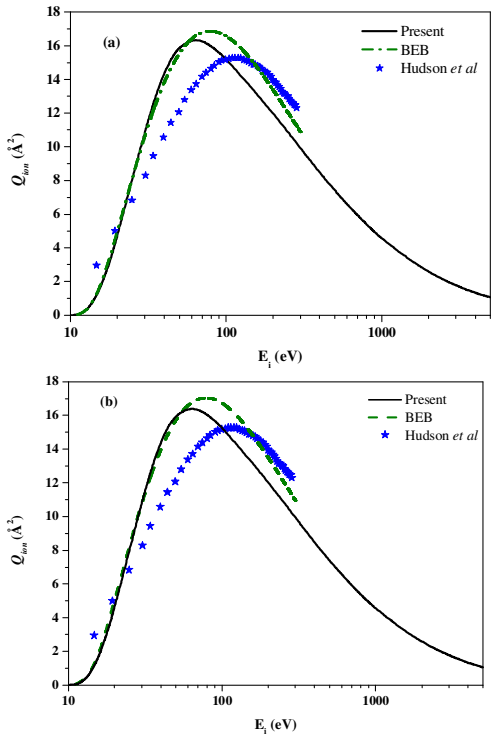

Fig 4. $\boldsymbol{Q_{ion}}$ for (a) n-$CH_3COOCH_2CH_2CH_3$ and (b) iso-$CH_3COOCH_2CH_2CH_3$ in Å^2

Figures 4 (a) and (b) presents the ionisation cross section for the isomers of propyl ethanoates namely n-proply ethanoate and iso-propyl ethanoate, along with the measurements of Hudson *et al* [6] and revised BEB data given by Bull *et al* [10]. The comparison of the present cross section shows similar trend with Hudson *et al*'s [6] experimental values as shown by its previous counterparts. However, the agreement with the BEB data [10] is excellent till around the peak for both the molecules. It is clear from Figs 4(a) and (b) that the ionisation cross section of the iso-propyl ethanoate is relatively higher at peak as compared to its long chain partner. Actually, isomers have the same chemical sum formula, but differ in the geometrical arrangement of the constituent of the molecule. This results in a slightly different molecular orbital structure for each isomer. We can view the total ionisation cross sections as a result of probability of removing an electron from an individual molecular orbital summed over all the molecular orbitals. The difference in molecular orbital structure of these isomers can lead to slightly different ionisation cross section.

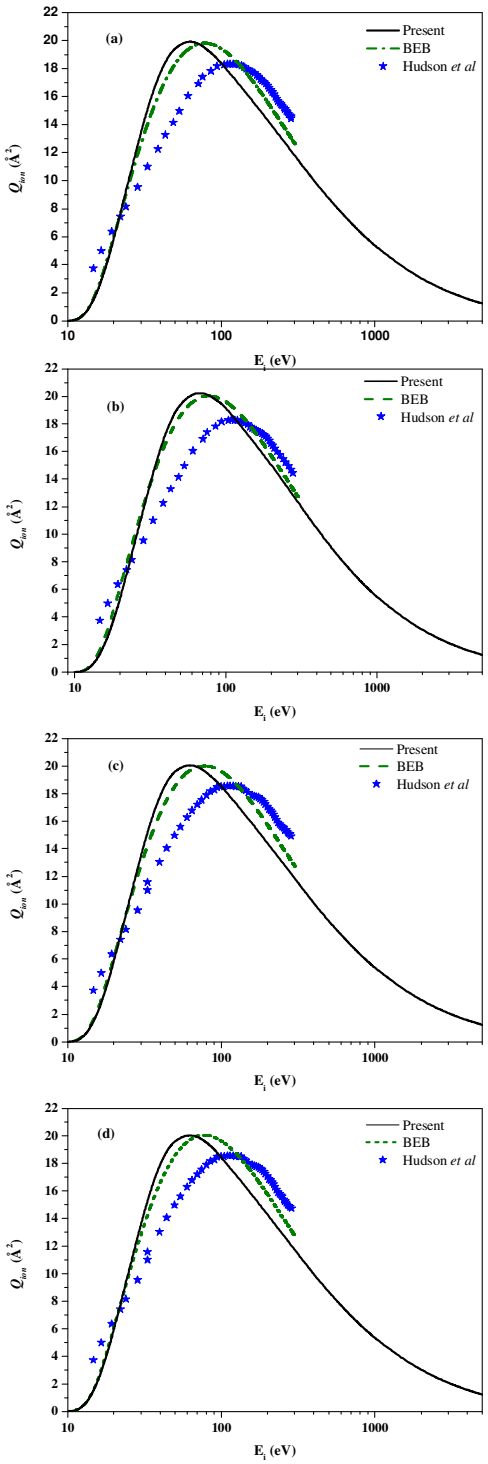

Fig 5. $\boldsymbol{Q_{ion}}$ for (a) $CH_3COOCH_2CH_2CH_2CH_3$ (b) sec-$CH_3COOCH_2CH_2CH_2CH_3$ (c) iso-$CH_3COOCH_2CH_2CH_2CH_3$ and (d) tert-$CH_3COOCH_2CH_2CH_2CH_3$ in Å^2

Figures 5(a)-(d) represent the ionisation cross sections for the isomers of butyl ethanoates with the available experimental and theoretical data. The present computational data compare quite well with the measurements of Hudson *et al* [6]. We can see that the shift in the position of present peak from the experimentally determined maximum ionisation cross section of Hudson *et al* [6] is quite consistent for the series of molecules studied here. Similar variation between the Q_{ion} computed by the present method and the experimental results of the same group [30, 31] was observed for the mono chloro alkane and chloro ethane molecules reported in our previous works [11, 32]. The consistent discrepancy between the present and experimental results for all the targets studied here is very interesting. It may be attributed to the experimental uncertainty in characterising the pure gas targets. The nature and shape of the present ionisation curve for all the ethanoates is found to be in close proximity to the measurements. The agreement between the present cross section with that of the BEB data [10] is excellent throughout. The present ionisation curve almost retraces the BEB curve for all the isomers of butyl ethanoate. It is observed that the ionisation cross section of n-butyl ethanoate is slightly different from its isomers. The difference is apparent at the peak position, which can be attributed to difference in molecular orbital structure of these isomers as explained for the isomeric case of propyl ethanoate.

Figure 6 shows Q_{ion} curves for all the ethanoate molecules studied in the present work. It appears that the addition of 8 electrons (an equivalent of a -CH_2 group) while moving up in the ethanoate hierarchy, the magnitude of the cross section increases considerably. This reflects the fact that the ionisation cross section increases with target size. Furthermore, we can see that the Q_{ion} for the isomers of a particular ethanoate almost overlap up to the peak, although beyond the peak a slight difference in the ionisation cross sections is observed. The characteristic at low incident energies is dependent mainly on the close ionisation thresholds. However, at high energies the behaviour is attributed to the difference in the orientation of molecular orbitals in these isomers.

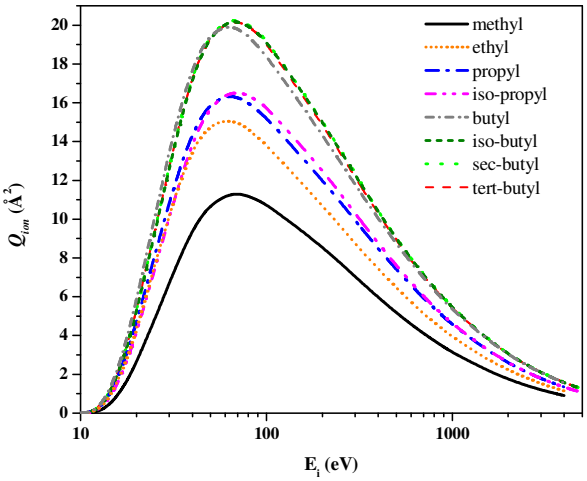

Fig 6. Q_{ion} plot of ethanoates

Table 5 Calculated polarisability from correlation plot (Fig. 7) for C_5 and C_6 ethanoates, including isomers.

Molecule	polarisability (Å^3)
propyl ethanoate	10.64
iso-propyl ethanoate	10.74
butyl ethanoate	13.70
sec-butyl ethanoate	13.83
iso-butyl ethanoate	13.79
tert-butyl ethanoate	13.82

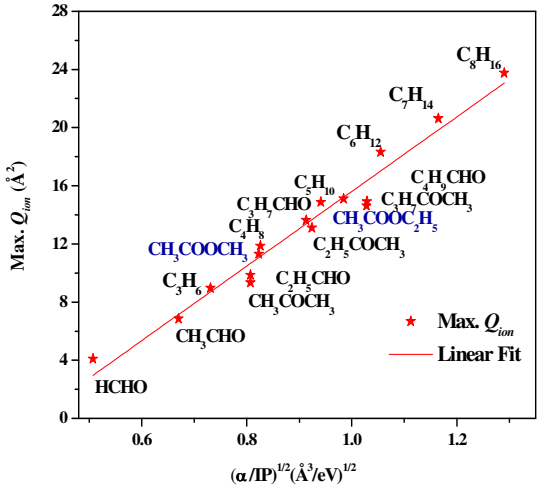

Fig 7. Correlation plot of Max. Q_{ion} with $(\alpha/IP)^{1/2}$

Table 6 Max. Q_{ion} of ethanoates from present and previous studies.

Molecule	SCOP+ CSP-ic	Correlation plot	Hudson *et al* [6]	BEB (Bull *et al*) [10]
methyl ethanoate	11.32	11.05	10.5	11.02
ethyl ethanoate	15.11	15.20	13.8	13.91
propyl ethanoate	16.36	-	15.7	16.86
iso-propyl ethanoate	16.56	-	15.2	17.03
butyl ethanoate	19.98	-	18.3	19.80
sec-butyl ethanoate	20.29	-	18.2	20.03
iso-butyl ethanoate	20.22	-	18.3	20.02
tert-butyl ethanoate	20.20	-	18.5	20.04

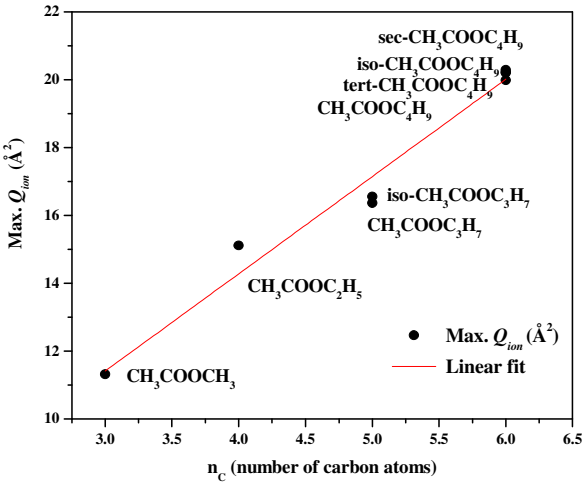

Fig 8. Plot of Max. Q_{ion} for ethanoates versus the number of carbon atoms in the molecule.

Harland and Vallance [33] have shown by simple electrostatic considerations that a strong correlation exists between the maximum electron impact ionisation cross section and the square root of the ratio of atomic or molecular polarisability volume to ionisation potential. This was later confirmed using experimental data from literature. Such correlations based on empirical and semi-empirical formulas are very useful and can be used as a precursor tool to test the theoretical predictions of cross sections. In Fig 7, we have presented the correlations between the maximum of total ionisation cross section with the square root of the ratio of polarisability volume to ionisation potential, $(\alpha/IP)^{1/2}$ for aldehyde, ketone and cyclohexane molecules already reported in a previous work [12]. It is encouraging to see that correlation between the present maximum of Q_{ion} for ethanoates versus $(\alpha/IP)^{1/2}$ (wherever α is available) fall close to the linear fit for aldehyde, ketone and cyclohexane molecules [12]. This fit provides a relation between the maximum Q_{ion} and $(\alpha/IP)^{1/2}$ for the ethanoates studied here. Therefore, such correlation can be used as an alternative route to estimate the unknown polarisability volumes. The polarisabilities for propyl and butyl ethanoates (including isomers) estimated in the present work using the correlation plot of Fig.7 are listed in Table 5. The knowledge of polarisability volumes are very important in the calculation of a range of physical parameters including: modelling of refraction by polar and non-polar molecules; the calculation of dielectric constants and diamagnetic susceptibility; ion mobility in gases; long-range electron–molecule and ion–molecule interaction energies; Langevin capture cross-sections and rate constants for polar and non-polar molecules; van der Waals constants; and oscillator strengths. The maximum total ionisation cross section estimate from the correlation plot for targets with known molecular parameters [34] (methyl and ethyl ethanoates) are also included in Table 6. Thus, we can verify that the correlation plot gives a proximate peak of ionisation cross section calculated by SCOP+CSP-ic and hence can be aptly used for roughly estimating the polarisabilities of other molecules of same family.

Figure 8 depicts the plot of maximum ionisation cross section for the ethanoates with the number of carbon atoms contained in the molecule. A linear fit trough the points suggests a linear relationship between the maximum Q_{ion} and the number of carbon

atoms for this series of molecules, which indicates that with the introduction of -CH_2 group in the alkyl part of ethanoates, there is a uniform increase in the cross section. Such correlations can be used to estimate the mean value of maximum ionisation cross section of higher members of ethanoate family by simple extrapolation.

IV. Conclusion

The present article reports the total ionisation cross sections for C_3 to C_6 ethanoates in the energy regime from ionisation threshold to 5 keV. SCOP and CSP-ic formalisms along with GAR method [11] are employed for the computation of the cross sections. We have obtained reliable cross sections for all the targets studied here. It is encouraging to see that the present ionisation cross section curves for the group of molecules studied here, show a consistent behaviour compared to the measurements of Hudson *et al.* [6]. This deviation may be due to the following reasons: (i) experimental uncertainties, (ii) difficulty in preparing pure target gas and/or (iii) resolution in incident energy beam. The peak of the present ionisation curve consistently lies at lower energy side relative to the experimental curve. This consistent variation suggests a systematic error in the measurement of cross sections or in the determination of incident energy beam.

A good agreement is observed between the ionisation cross sections reported here and BEB data [10]. DM [18] calculations for methyl and ethyl ethanoates show good accord with the present results at energies up to the peak, although beyond that significant deviation is observed. Dependence of isomeric effect to the electron impact cross section was also investigated. We have obtained slightly different ionisation cross sections for the isomers of ethanoate due to the difference in their geometry and ionisation potential of these compounds. In Fig. 7, a strong correlation between the maximum ionisation cross section with square root of the ratio of polarisability to ionisation potential is observed. This linear relationship establishes the fact that the cross sections calculated are consistent and reliable and can be employed in relevant areas of applied interest. Such correlations could also be further used for the estimation of molecular parameters like polarisability volume or ionisation potential when either of them is unknown for a molecule. Using this correlation plot, a reasonable estimate of polarisability volumes for C_5 and C_6 ethanoates are determined for the first time, albeit approximate.

Acknowledgement

BKA is pleased to acknowledge the support of this research by the Department of Science and Technology (DST), New Delhi through Grant No. SR/S2/LOP-11/2013.

Notes and references

Atomic & Molecular Physics Group, Department of Applied Physics, Indian School of Mines, Dhanbad, 826004, Jharkhand, India. Tel: +91 9470194795; E-mail: bka.ism@gmail.com

1 Robert S. Freund, Swarm Studies and Inelastic Electron-Molecule Collisions,1987, pp 329-346 .
2 B. Tercero, I. Kleiner, J. Cernicharo, H. V. L. Nguyen, A. López, and G. M. Muñoz Caro, *ApJ*, 2013, 770, L13.
3 R. T. Garrod, S. L. W. Weaver and E. Herbst, *ApJ*, 2008, 682, 283.
4 B. Sivaraman, B. G. Nair, J. -I. Lo, S. Kundu, D. Davis, V. Prabhudesai, B. N. Raja Sekhar, N. J. Mason, B. -M. Cheng, and E. Krishnakumar, *ApJ*, 2013, 778(2), 157.
5 A. G. Harrison, E. G. Jones, S. K. Gupta, G. P. Nagy, *Can. J. Chem.*, 1966, 44, 1967-1973.
6 J. E. Hudson, Ze F. Weng , C. Vallance and P. W. Harland, *Int. J. of Mass Spectrom.*, 2006, 248, 42–46.
7 Y. K. Kim, M. E. Rudd, *Phys. Rev. A*, 1994, 50, 3954.
8 W. Hwang, Y. K. Kim and M. E. Rudd, *J. Chem. Phys.*, 1996, 104, 2956.
9 H. Deutsch, and T. D. Mark, *Int. J. Mass. Spectrom. Ion Proc.* 1987, 79, R1-R8.
10 J. N. Bull, P.W. Harland and C. Vallance, *J. Phys. Chem. A*, 2012, 116, 767–777.
11 R. Naghma, D. Gupta, B. Goswami, B. K. Antony, *Int. J. Mass Spectrom.*, 2014, 360, 39.
12 D. Gupta, B. K. Antony, *J. Chem. Phys.*, 2014, 141, 054303.
13 B. Goswami, R. Naghma and B. K. Antony, *RSC Adv.*, 2014, 4, 63817-63823.
14 M. Vinodkumar, A. Barot, and B. K. Antony, *J. Chem. Phys.*, 2012, 136, 184308.
15 M. Vinodkumar, H. Bhutadia, B. K. Antony and N. J. Mason, *Phys. Rev. A*, 2011, 84, 052701.
16 D. Gupta, R. Naghma, B. Goswami and B. K. Antony, *RSC Adv.*, 2014, 4, 9197-9204.
17 B. Goswami and B. K. Antony, *RSC Adv.*, 2014, 4, 30953-30962.
18 Private communication, Claire Vallance.
19 http://www.indsci.com/docs/manuals/VX500_IP.pdf.
20 Website: http://www.cccbdb.nist.gov/.
21 H.L. Cox and R.A. Bonham, *Chem. Phys.*, 1967, 47, 2599 .
22 S. Hara, *J. Phys. Soc. Jpn.*, 1967, 22, 710.
23 X. Zhang, J. Sun and Y. Liu, *J. Phys. B*, 1992, 25, 1893.
24 G. Staszewska, D. W. Schwenke, D. Thirumalai and D. G. Truhlar, *Phys. Rev. A*, 1983, 8, 2740.
25 J. E. Turner, H. G. Paretzke, R. N. Hamm , H. A. Wright and R. H. Richie, *Radiat. Res.*, 1982, 92, 47.
26 G. P. Karwasz, R. S. Brusa and A. Zecca, *Nuovo Cim.*, 2001, 24, 1.
27 M. Vinodkumar, C. Limbachiya, B. K. Antony and K. N. Joshipura, *J. Phys. B: At. Mol. Opt. Phys.*, 2007, 40, 3259–3271.
28 K. N. Joshipura, B. K. Antony and M. Vinodkumar, *J. Phys. B: At. Mol. Opt. Phys.* , 2002, 35, 4211–422.
29 K. N. Joshipura and M. Vinodkumar, *J. Phys. B: At. Mol. Opt. Phys.*, 2001, 34, 509.
30 J. E. Hudson, C. Vallence, M. Bart and P. W. Harland, *J. Phys. B: At. Mol. Opt. Phys.*, 2001, 34, 3025.
31 M. Bart, P. W. Harland, J. E. Hudson and C. Vallence, *Phys. Chem. Chem. Phys.*, 2001, 3, 800.
32 R. Naghma and B. K. Antony, *Int. J. Mass Spectrom.*, 2014, 373, 34-38.
33 P. W. Harland, C. Vallance, Int. J of Mass Spectrom. and Ion Processes, 1991, 171, 173-181.
34 David R. Lide, ed., CRC Handbook of Chemistry and Physics, Internet Version 2005, CRC Press, Boca Raton, FL, 2005.